Rapid production of new oligodendrocytes is required in the earliest stages of motor skill learning

Lin Xiao[1, 2, 5], David Ohayon[1, 4, 5], Ian A. McKenzie[1], Alexander Sinclair-Wilson[1], Jordan L. Wright[1], Alexander D. Fudge[1], Ben Emery[3], Huiliang Li[1, 6] and William D Richardson[1, 6, 7]

[1] Wolfson Institute for Biomedical Research, University College London, Gower Street, London, WC1E 6BT

[2] Institute of Neuroscience, Second Military Medical University, 800 Xiangyin Road, Shanghai 200433, China

[3] Jungers Center for Neurosciences Research, Oregon Health and Science University, 3181 SW Sam Jackson Park Road, Portland, OR 97239-3098

[4] present address: Centre de Biologie du Développement, University Paul Sabatier, 118 route de Narbonne, 31062 Toulouse, CEDEX 9, France

[5] equal contributions [6] joint senior authors [7] corresponding author

Correspondence to: w.richardson@ucl.ac.uk tel +44 (0)20 7679 6729

Key words: motor learning, motor performance, skill learning, glia, oligodendrocyte, precursor cell, NG2 cell, myelin, white matter, mouse

Summary *(146 words)*

We identified a novel marker of newly-forming oligodendrocytes – the ecto-enzyme Enpp6 – and used this to track oligodendrocyte differentiation in adult mice as they learned a motor skill (running on a wheel with unevenly spaced rungs). Production of *Enpp6* -expressing immature oligodendrocytes was accelerated within just 2.5 hours exposure to the complex wheel in subcortical white matter and within 4 hours in motor cortex. Conditional deletion of *Myelin regulatory factor (Myrf)* in oligodendrocyte precursors blocked formation of new *Enpp6*$^{+}$ oligodendrocytes and impaired learning within the same ~2-3 hour time frame. This very early requirement for oligodendrocytes suggests a direct and active role in learning, closely linked to synaptic strengthening. Running performance of normal mice continued to improve over the following week accompanied by secondary waves of oligodendrocyte precursor proliferation and differentiation. We conclude that new oligodendrocytes contribute to both early and late stages of motor skill learning.

In the vertebrate central nervous system (CNS) many axons are ensheathed by myelin – tight spiral wraps of plasma membrane made by oligodendrocytes. Myelin greatly increases the speed of propagation of action potentials, permitting rapid information transfer over long distances and allowing the evolution of larger animals with bigger, more powerful brains. Approximately 5% of all neural cells in the rodent and human brain are oligodendrocyte precursors (OPs). These glial precursors generate the majority of myelinating oligodendrocytes during the early postnatal period (the first ~10 weeks in mice and 5-10 years in humans)[1,2], but continue to generate oligodendrocytes and myelin at a declining rate subsequently[2-9]. Differentiation of OPs into oligodendrocytes depends on the transcription factor Myelin regulatory factor (Myrf)[10,11]. Myrf is not expressed in cycling OPs but is first transcribed in differentiating oligodendrocytes, in which it is required for activation of many downstream genes including those encoding myelin structural proteins[10-12].

We previously investigated the function of adult-born oligodendrocytes in mice by inactivating *Myrf* conditionally in OPs, using tamoxifen-inducible CreER^{T2} under *Platelet-derived growth factor receptor-alpha* transcriptional control (*Pdgfra-CreER*^{T2}) to recombine and delete a "floxed" allele of *Myrf* [*P-Myrf*$^{-/-}$ mice][13]. This dramatically reduced new oligodendrocyte production from their precursors without affecting pre-formed oligodendrocytes or myelin – and prevented mice from mastering a new motor skill (running on a "complex wheel" with irregular rung spacing). We concluded that development of new oligodendrocytes during adulthood is required for motor

learning[13]. However, their precise role in the learning mechanism remains unclear. They might be needed in a purely permissive role – for example, to repair myelin that is lost or damaged in use, so that the underlying neural circuitry remains competent for learning. Alternatively, they might be involved more directly. For example, they might improve conduction by synthesizing myelin, by inducing sodium channels to cluster at "pre-nodes" prior to myelination [21], or by transferring substrates for energy production (lactate and pyruvate) into axons [22,23]. Any or all of these mechanisms might improve the performance of new circuits while preserving them for future use.

A key component of learning at the subcellular level is synaptic modification[14-17]. This can occur very rapidly; there are dynamic changes to the number and size of dendritic spines (sites of synaptic contact) on pyramidal neurons in the mouse motor cortex within one-and-a-half hours of initiating fine-motor training[18]. This is much faster than previously reported responses of oligodendrocyte lineage cells to novel experience[13], or to other physiological or artificial stimuli [8,13,19,20], which have been reported to occur over days to weeks. This might suggest that oligodendrocytes act far downstream of synaptic change or in an entirely separate pathway. However, our knowledge of how oligodendrocyte lineage cells change in response to novel experience is still rudimentary and more work is required before we can understand their role in neural plasticity.

To help elucidate the contribution of oligodendrocytes to motor learning, we have now examined the time course of learning and the accompanying cellular events at higher temporal resolution than before. We analyzed complex wheel-running data for *P-Myrf* $^{-/-}$ mice and their *P-Myrf* $^{+/-}$ littermates and discovered – quite unexpectedly – that the performance of the two groups diverged very early, within 2-3 hours of their being introduced to the wheel. This result implies that oligodendrocyte differentiation is required at a very early stage of motor skill learning, close to the point at which synaptic change occurs[18], suggesting that oligodendrocytes and myelin play a more active role in learning and memory than might have been imagined previously.

To look for direct evidence of early involvement of oligodendrocyte lineage cells we analyzed OP proliferation and differentiation in the motor cortex and subcortical white matter of wild type mice during the early stages of learning. Remarkably, using a novel molecular marker Enpp6 (a choline-specific ecto-nucleotide pyrophosphatase/ phosphodiesterase)[24-26] that is preferentially expressed in early-differentiating oligodendrocytes (reference 27 and this paper), we were able to detect accelerated differentiation of OPs into newly forming oligodendrocytes after just 2.5 hours self-training on the complex wheel. This early phase of oligodendrocyte production presumably involves direct differentiation of OPs that were paused in the G1 phase of the cell cycle before the

wheel was introduced. The sudden surge of differentiation resulted in a transient dip in the local density (cells/ mm^2) of OPs followed by increased S-phase entry among the remaining OPs and elevated oligodendrocyte production in the longer term (>10 days). Thus, it appears that a primary effect of novel experience is to stimulate rapid differentiation, within hours, of G1-arrested OPs into new oligodendrocytes that participate in and are required for optimal early-stage learning. The subsequent wave of OP proliferation and differentiation, presumably a homeostatic reaction to the initial depletion of OPs[28], occurs together with continuing improvement in running performance, suggesting that the later-generated oligodendrocytes also contribute to learning and long-term motor memory.

Results

Myrf is required in the first few hours of skill learning

We analyzed the ability of mice to run at speed on a "complex wheel" with irregularly spaced rungs, as described previously[13]. We assembled a large dataset from tamoxifen-treated *Pdgfra-CreER^{T2}: Myrf$^{flox/flox}$* mice (referred to as *P-Myrf $^{-/-}$*) and their *P-Myrf $^{+/-}$* littermates [n= 32 (17 males) and n=36 (20 males), respectively], by combining data from several smaller cohorts of one or two litters each (P60 or P90 at the time of running). Mice ran mainly during the dark/night cycle (6pm-6am) and were inactive in the day. As reported previously, both *P-Myrf $^{+/-}$* and *P-Myrf $^{-/-}$* mice improved their running speeds over a period of about one week, but the average or maximum speeds attained by *P-Myrf $^{-/-}$* mice were always less than the control *P-Myrf $^{+/-}$* group (reference 13 and Fig. 1a; all mice received tamoxifen on four consecutive days, three weeks before running). At the end of the first night the performances of the two groups had already diverged, implying that Myrf-dependent processes were important during the first 12 hours for optimal learning. Plotting average speed over successive 2-hour (rather than 12-hour) intervals showed that for both *P-Myrf $^{-/-}$* and control groups most improvement during the first night occurred within the first 4 hours, after which running performance leveled off (Fig. 1b). At the beginning of the second night, following 12 hours of daytime inactivity and sleep, performance was immediately better than it had been at any time in the previous 24 hours (Fig. 1b). This mirrors the sleep-dependent "consolidation" that is observed in humans learning a motor task[30]. On subsequent nights performance improved incrementally from one night to the next, beginning at a level close to the previous night's peak and improving further for a few hours before tailing off (Fig. 1b and Supplementary Fig. 1).

Plotting average speed over 20-minute intervals revealed, remarkably, that the performance of *P-Myrf $^{-/-}$* mice was already impaired relative to their *P-Myrf $^{+/-}$* littermates within the first 2-3 hours of the first night (Fig. 1c). This early requirement for Myrf presumably reflects

differentiation of *Pdgfra*-expressing OPs into new oligodendrocytes; it cannot reflect modification or adaptation of pre-existing oligodendrocytes or myelin because differentiated oligodendrocytes do not express *Pdgfra-CreER*^{T2} and therefore do not delete *Myrf* ^{flox}. OPs lacking *Myrf* do not differentiate properly but arrest and die before the expression of myelin structural genes[10,11,13].

Motor training accelerates OP differentiation

This rapid improvement in motor performance far precedes the running-induced OP proliferation that we detected at 2-4 days in our previous study[13] (see Introduction). However, in that study we administered the nucleotide analogue 5-ethynyl-2'-deoxyuridine (EdU) from the time mice first encountered the wheel, so we could follow the fates only of those cells that entered S-phase after that point. That could have limited our ability to detect the earliest cellular responses. Therefore, in a new set of experiments we *pre-labeled* wild type mice with EdU for ten days – from postnatal day 75 (P75) to P85 – *prior to* introducing the wheel (Fig. 2a). This was sufficient to label ~20% of OPs in the cortical gray matter and ~75% of OPs in the subcortical white matter (not shown). We then followed the fates of those EdU-labeled cells in mice that had self-trained on the wheel for 48 hours (P85–87), by co-immunolabeling for Pdgfra to identify OPs and with monoclonal CC1 for oligodendrocytes. The great majority of EdU$^+$ cells in both gray and white matter was also Sox10$^+$ (96.7% ± 0.6%; >1000 cells counted in >3 sections from each of 3 mice, Fig. 2b) so EdU labeling can be used as a proxy oligodendrocyte lineage marker in these experiments. Unexpectedly, there was a *reduction* in the number density of (EdU$^+$ Pdgfra$^+$) OPs in mice housed with a wheel ("runners") relative to littermates without a wheel ("non-runners") both in the motor cortex (7.3 ± 0.6 cells/ mm^2 versus 10.4 ± 0.7 in runners versus non-runners; p=0.01) and in sub-cortical white matter (71.2 ± 6.2 versus 91.9 ± 4.0 cells/ mm^2; p=0.02. ≥3 sections analyzed from each of 6 mice, two-tailed unpaired *t*-test) (Fig. 2c, d). This was accompanied by a reciprocal *increase* in the number density of EdU$^+$, Sox10$^+$, Pdgfra/CC1 double-negative cells – that is, newly-differentiating oligodendrocytes that had lost Pdgfra but not yet acquired CC1 immunoreactivity (Motor cortex: 4.1 ± 0.5 versus 2.3 ± 0.2 cells/ mm^2 in runners and non-runners; p=0.01. Subcortical white matter: 73.5 ± 8.9 versus 51.0 ± 5.5 cells/ mm^2; p=0.03) (Fig. 2c, d). These data demonstrate that novel experience with the complex wheel stimulates differentiation of OPs that had replicated their DNA in the 10 days before introduction to the wheel. At this time point (2 days with the wheel) there was no difference in the density of (EdU$^+$ CC1$^+$) oligodendrocytes in runners versus non-runners (Figs 2c–e). However, a significant increase developed in runners between 2 and 4 days – both in the motor cortex and subcortical white matter – and these increases persisted beyond 8 days (Fig. 2e, f). Numbers of (EdU$^+$ CC1$^+$) newly-formed oligodendrocytes were much reduced in *P-Myrf* $^{-/-}$ mice (p<0.10^{-4}), as expected (Fig. 2e, f). There was no increase in oligodendrocyte

production in the optic nerves of runners versus non-runners (Fig. 2g), demonstrating regional specificity of the response.

Enpp6, a novel marker of newly-forming oligodendrocytes

These cellular responses to wheel running after 2 days were still much delayed relative to the 2-3 hours required to register an improvement in running performance (Fig. 1c). Nevertheless, the results described above drew our attention to the potential role of OP differentiation in early stages of learning. To facilitate study of early OP differentiation we scanned existing expression databases for developmental stage-specific markers and identified a gene, *Enpp6*, that is expressed highly in newly forming oligodendrocytes and at a much lower level in more mature myelinating oligodendrocytes, but not at all in OPs, neurons, astrocytes, or vascular endothelial cells[27] (Fig. 3a). In situ hybridization (ISH) for *Enpp6* labeled cells in both the grey and white matter of the P60 mouse brain (Supplementary Fig. 2). Two populations of *Enpp6*$^{+}$ cells were detected; the majority had small, weakly-labeled cell bodies but a minor sub-population was larger and more intensely-labeled (Fig. 3b; Supplementary Fig. 2). This expression pattern is consistent with the interpretation that the numerous weakly-labeled cells are mature oligodendrocytes, while the less abundant strongly-labeled cells are newly-differentiating, in keeping with the RNA-seq data[27].

Under appropriately adjusted ISH conditions we were able to filter out the weakly-labeled cells and visualize only the strongly-labeled, putative newly-differentiating oligodendrocytes (Supplementary Fig. 2b). These *Enpp6*^{high} cells do not express *Pdgfra* – so they are not OPs – but they all express Sox10 and/or Olig2 immunoreactivity (Supplementary Fig. 2c, Supplementary Fig. 3, Supplementary Table 1). Most but not all of them co-labeled with CC1 (Supplementary Fig. 3; Supplementary Table 1) and they all express *Myelin basic protein* (*Mbp*) mRNA (Fig. 3b, c; Supplementary Table 1), identifying them as oligodendrocytes. At P90 the (*Enpp6*^{high} *Mbp*$^{+}$) cells had a distinctive "spidery" morphology with multiple radial processes (Fig. 3b, c). All *Enpp6*^{high} cells were *Mbp*$^{+}$spidery cells and vice versa (Fig.3c; Supplementary Table 1) and were <5% of all *Mbp*$^{+}$ oligodendrocytes at P90. The (*Enpp6*^{high} *Mbp*$^{+}$) spidery cells were practically absent from *P-Myrf*$^{-/-}$ brains (compare Fig. 3d, e), confirming that they are newly-forming oligodendrocytes [13]. A morphological sub-class of oligodendrocyte resembling the (*Enpp6*^{high} *Mbp*$^{+}$) cells and described as "pre-myelinating" has been visualized previously in rodent and human brains, by immunolabeling for the myelin Proteolipid protein (Plp, DM20 isoform) [31,32].

We found that in P10 cerebral cortex, ~45% (66/146) of (*Enpp6*^{high} *Mbp*$^{+}$) cells co-expressed the myelin structural proteins Myelin-associated glycoprotein (Mag) and Mbp in their cell bodies and

processes, including myelin sheaths (Fig. 4a). Some of these (e.g. cell 1 in Fig. 4a) expressed low amounts of Mbp protein, suggesting that they were newly-myelinating. Those that expressed higher amounts of Mbp (e.g. cell 2 in Fig. 4a) tended to express low levels of *Enpp6*, consistent with *Enpp6* being down-regulated as oligodendrocytes mature. Many *Enpp6*$^{+}$ cells co-expressed *Mbp* mRNA in their cell bodies as well as in their Mbp protein-positive myelin sheaths, both at P10 and P90 (Fig. 4b–d). At P90, in layer 2 of the motor cortex where myelin internodes were less dense and easier to to associate with individual cell bodies, ~65% (37/55) of (*Enpp6*^{high} *Mbp*$^{+}$) cells clearly co-expressed Mbp protein (Fig 4c, d). We conclude that a significant fraction of *Enpp6*^{high} cells in developing and adult brains synthesize nascent myelin sheaths.

The distribution pattern of *Enpp6*^{high} cells in the developing brain was distinct from either *Pdgfra*$^{+}$ OPs or the general population of *Mbp*$^{+}$ or *Plp*$^{+}$ oligodendrocytes (Fig. 5a–c). They were almost completely absent from *P-Myrf*$^{-/-}$ brains (Fig. 5d) – further confirmation that they are oligodendrocyte lineage cells. The number of *Enpp6*^{high} cells declined markedly with age, in keeping with the diminishing rate of oligodendrocyte differentiation[9] (Fig. 5e–h). *Enpp6*^{high} newly-differentiating oligodendrocytes were still evident in the corpus callosum and cerebral cortex of young adult (P90) mice (Fig. 5g) and even at P365 small numbers of these cells could be detected (Fig. 5h), consistent with a low rate of new oligodendrocyte production even at one year of age.

Enpp6 starts to be expressed after Pdgfra is extinguished and overlaps with the onset of CC1 expression, but is down-regulated in more mature myelinating oligodendrocytes, which continue to express CC1 (Supplementary Figs. 2, 3; Supplementary Table 1). Therefore, *Enpp6*^{high} cells include some but not all (Pdgfra^{-} CC1^{-}) early-differentiating oligodendrocytes (Fig. 2), as well as the earliest-forming CC1^{+} oligodendrocytes.

Accelerated production of Enpp6^{+} cells during training

We used in situ hybridization for *Enpp6* mRNA to detect newly differentiating oligodendrocytes in mice that were learning to run on the complex wheel (Fig. 6a–i). Remarkably, within just 2.5 hours we could detect an increase in the number of *Enpp6*^{high} cells in the subcortical white matter of runners versus non-runners (35.9 ± 2.0 versus 28.4 ± 1.7 cells/mm^2 in runners vs non-runners; p=0.003. ≥3 sections from each of 8 mice) (Fig. 6k). This increase in cell number occurs on the same time-frame as the earliest improvements in running performance (Fig. 1c), arguing that new oligodendrocyte production is an integral part of early-stage motor learning, occurring in parallel with, or closely following, changes at the level of synapses[18]. At 2.5 hours we could detect no change in *Enpp6*^{high} cells in the motor cortex of runners versus non-runners (Fig. 6j). However, at

4 hours there was a ~25% increase in *Enpp6*^{high} cells in both motor cortex and subcortical white matter (Motor cortex: 12.9 ± 0.4 versus 9.6 ± 0.6 cells/ mm^2 in runners vs non-runners; p<0.001. Subcortical white matter: 40.5 ± 2.5 vs 29.4 ± 2.5 cells/ mm^2; p=0.003. ≥3 sections from each of 10 mice). After 12 hours (one night) with the wheel there was a ~50% increase in *Enpp6* ^{high} cells in runners versus non-runners (Motor cortex: 15.7 ± 0.6 vs 9.6 ± 0.4 cells/ mm^2; p<0.001. Subcortical white matter: 48.7 ± 2.4 vs 29.4 ± 1.7 cells/ mm^2; p<0.001) and after another 12 hours (i.e. one night plus the following daytime/ inactivity period) an even larger (~2-fold) increase (Motor cortex: 23.3 ± 1.2 vs 10.7 ± 1.1 cells/ mm^2; p<0.001. Subcortical white matter: 54.2 ± 7.9 vs 27.9 ± 2.2 cells/ mm^2; p<0.001) (Fig. 6j, k). These latter data raise the possibility that the improvement in running performance that develops during sleep/ inactivity (Fig. 1c) might be related to ongoing oligodendrocyte generation; it has been reported that OP proliferation and differentiation is circadian, S-phase entry occurring preferentially during the day, M-phase and oligodendrocyte differentiation at night[33,34]. Production of *Enpp6* ^{high} cells was dramatically reduced in *P-Myrf* $^{-/-}$ mice relative to wild type mice both in non-runners and 12-hour runners (Fig. 6c, f, i-k), as expected. Increased numbers of newly-formed *Enpp6*^{high} oligodendrocytes were still observed in 8-day runners, though in reduced numbers compared to earlier times (Fig. 6j, k).

Motor learning, not exercise, stimulates oligodendrogenesis

Increased oligodendrocyte differentiation might conceivably have been part of a systemic response to exercise, rather than to motor learning per se. To disentangle these effects we compared two cohorts of wild type mice, one of which self-trained on the complex wheel for eight days, rested for two weeks, then was re-introduced to the complex wheel for 24 hours. The other cohort was introduced to the complex wheel once only, for 24 hours (Fig. 7a). The average running speed and distance travelled over 24 hours of the “first-timers" was much less than the “second timers” that had already mastered the wheel two weeks previously (Fig. 7b, c). Despite this, the *Enpp6* ^{high} number density was increased in motor cortex and underlying white matter *only* in the first-timers (Fig. 7d, e). This experiment dissociates running speed (physical exercise) from novel running experience (learning) and demonstrates that the rate of production of new oligodendrocytes is increased only during the primary learning event. Moreover, increased production of *Enpp6* ^{high} newly-differentiating oligodendrocytes was induced in motor cortex but not visual cortex of the first-timers in this experiment (Fig. 7f), demonstrating regional specificity of the early learning response.

Discussion

We have presented evidence that oligodendrocyte development is required for motor learning in adult mice, within the first few hours of their being introduced to the complex running wheel. The performance of *P-Myrf* $^{-/-}$ and *P-Myrf* $^{+/-}$ groups both started out at baseline, but they improved at different rates over the first 2-3 hours before equilibrating at different levels. This observation reinforces our conclusion that the two groups learn at different rates, rather than possessing inherently different physical abilities, since the physical effort required for this initial low speed wheel-turning is unlikely to be limiting. At the cellular level, the primary response is accelerated production of (*Enpp6*$^{+}$ *Mbp*$^{+}$) early-differentiating ("spidery") oligodendrocytes, which was detected already within the first 2.5 hours (see diagram in Supplementary Fig. 4). This might underestimate the rapidity of the response, since *Enpp6* does not mark the very earliest-differentiating cells – there is still a gap between down-regulation of *Pdgfra* and appearance of *Enpp6* (Supplementary Fig. 4). The rapid increase in *Enpp6*$^{+}$ newly-forming oligodendrocytes is likely to result from stimulated differentiation of G1-paused OPs, because at 2 days of training we observed a reduction in the absolute number of OPs (Fig. 2c, d); however, it is possible that increased survival of *Enpp6*$^{+}$ cells also plays a part. Production of *Enpp6* ^{high} newly-forming oligodendrocytes peaked around 24 hours and declined thereafter, although increased production was still evident after 8 days. This peak of new oligodendrocyte production was observed only during the first encounter with the wheel, not a subsequent encounter and only in motor, not visual cortex - suggesting that it is a specific response to motor learning, not exercise per se.

The early surge of OP differentiation was reflected in a reduction at 2 days running in the number of OPs (pre-labeled with EdU) and a corresponding increase in the number of (Pdgfra^{-} CC1^{-}) newly-forming oligodendrocytes. This was followed at 2–4 days by accelerated S-phase entry of some of the remaining OPs[13]. This sequence suggests that the S-phase entry observed at 2–4 days is a homeostatic response to the earlier depletion of OPs through differentiation. For example, local depletion of OPs could result in loss of contact inhibition[28] or a local excess (through reduced consumption) of a mitogenic growth factor (e.g. Pdgf)[35], either or both of which might stimulate proliferation of the remaining OPs in the locality. This spike of OP generation propels a secondary wave of oligodendrocyte production over the following days to weeks (Figs. 2d; Fig. 4g, h and reference 13). The dynamics of the system are complex and it seems likely that oligodendrocytes contribute to motor skill acquisition in different ways at different stages of the process.

Various learning regimens in humans and rodents are associated with changes to the microstructure of grey and white matter, detected by magnetic resonance diffusion tensor imaging (DTI). For

example, people or rats learning a complex visuomotor skill (e.g. juggling or abacus use for humans, food pellet grasping for rats) develop altered microstructure in the motor cortex and/or subcortical white matter after training for days to weeks[36-39]. Changes to gray and white matter microstructure can be detected even within 2 hours in people learning to play an action video game[40]. Experience-dependent structural changes to gray and/or white matter could in principle result from synaptogenesis and elaboration of the dendritic arbor[14-18], alterations to astrocyte morphology and their interactions with neurons[41], changes to the microvasculature[42] or altered (adaptive) myelination[19,20,43,44]. The results of our own present and previous studies[13] support the latter possibility.

Our ability to detect early oligodendrocyte dynamics relied partly on Enpp6, which we characterized as a novel marker of early-differentiating oligodendrocytes. Enpp6 is likely to become a useful new tool for studying oligodendrocyte differentiation in vivo e.g. during remyelination of demyelinated lesions. Enpp6 is considered to be a choline-specific glycerophosphodiester phosphodiesterase, since it can hydrolyze glycerophosphocholine and sphingosylphosphocholine efficiently in vitro[24-26]. Therefore, it seems likely that Enpp6 plays a role in lipid metabolism during formation of the myelin sheath and might be required to initiate myelination rapidly in response to differentiation-inducing signals, including those that operate during motor learning. It will be interesting in future to examine the functional role of Enpp6 and related family members during myelination.

How might newly-forming oligodendrocytes contribute to learning? The rapidity of their formation suggests that they work in close partnership with neurons, hand-in-hand with (or close on the heels of) synaptic change – not simply by preserving or "ossifying" new circuits after they have become established. For example, when mice first encounter the complex wheel they try to develop strategies for coping with unequal rung spacing; this presumably involves exploratory firing of distinct neurons or groups of neurons along the motor pathways. There might be several or many parallel circuits that can generate behavioural outputs within a useful range, some more effective than others. The superior circuit(s) might be activated more frequently than others as the action is rehearsed and so become selected and strengthened according to Hebbian principles – both at the level of the synapse and by rapid and selective myelination of the interconnecting axons. It is known that OPs receive synaptic input from axons (reviewed in reference 45) and that oligodendrocyte development and myelination can be regulated by axonal activity in vivo[19,20,43-47]. Newly-differentiating oligodendrocytes might enhance circuit function by initiating myelination and/or clustering of sodium channels and other nodal components prior to myelination [21], or by

supporting axonal metabolism[22,23], or a combination of those effects. This in turn could further enhance connectivity at the synaptic level and so on, back and forth. As myelin thickness and compaction increases, the performance of the network and its behavioural outputs would be expected to improve further. Therefore, oligodendrocytes are likely to contribute to learning over an extended period from hours to weeks. Ultimately, myelin protects axons metabolically and physically over the long term, preserving lifelong memories.

Acknowledgements

We thank our colleagues at UCL - especially Sarah Jolly, Ursula Grazini and Lorenza Magno - for advice and reagents, Matthew Grist and Ulla Dennehy for technical help. We thank Michael Wegner (University of Erlangen, Germany) for a gift of Sox10 antibody. This work was supported by the European Research Council (grant agreement 293544 to W.D.R.), the Wellcome Trust (100269/Z/12/Z to W.D.R.) and the Biotechnology and Biological Sciences Research Council (BB/L003236/1 to H.L.). L.X. was supported by the National Natural Science Foundation of China (grant 31471013). *Pdgfra-CreER*^{T2} mice can be obtained through www.e-lucid.com/ with a material transfer agreement. *Myrf* ^{flox} mice are available from Jackson Labs, strain 010607.

Author contributions

W.D.R. formed the hypotheses and obtained funding. I.A.M. adopted and developed the complex wheel test. B.E. provided *Myrf* ^{flox} mice, advice and suggestions. W.D.R., I.A.M. and D.O. designed the experiments in Fig. 1 and Fig. S1; D.O. and I.A.M. performed those experiments and DO analyzed the data. W.D.R., H.L. and L.X. designed all the other experiments and L.X. performed them, with assistance from A.S.-W., J.L.W. and A.D.F. H.L. identified *Enpp6* and AF performed preliminary characterization. H.L. and W.D.R. co-supervised the work. W.D.R. wrote the paper with input from H.L., L.X. and B.E.

Competing interests

The authors declare no competing financial interests.

References

1. Sturrock, R.R. Myelination of the mouse corpus callosum. *Neuropathol Appl Neurobiol* **6**, 415-420 (1980).

2. Yeung, M.S. *et al.* Dynamics of oligodendrocyte generation and myelination in the human brain. *Cell* **159**, 766-774 (2014).

3. Dimou, L., Simon, C., Kirchhoff, F., Takebayashi, H. & Gotz, M. Progeny of Olig2-expressing progenitors in the gray and white matter of the adult mouse cerebral cortex. *J Neurosci* **28**, 10434-10442 (2008).

4. Rivers, L.E. *et al.* PDGFRA/NG2 glia generate myelinating oligodendrocytes and piriform projection neurons in adult mice. *Nat Neurosci* **11**, 1392-1401 (2008).

5. Lasiene, J., Matsui, A., Sawa, Y., Wong, F. & Horner, P.J. Age-related myelin dynamics revealed by increased oligodendrogenesis and short internodes. *Aging Cell* **8**, 201-213 (2009).

6. Kang, S.H., Fukaya, M., Yang, J.K., Rothstein, J.D. & Bergles, D.E. $NG2^+$ CNS glial progenitors remain committed to the oligodendrocyte lineage in postnatal life and following neurodegeneration. *Neuron* **68**, 668-681 (2010).

7. Zhu, X. *et al.* Age-dependent fate and lineage restriction of single NG2 cells. *Development* **138**, 745-753 (2011).

8. Simon, C., Gotz, M. & Dimou, L. Progenitors in the adult cerebral cortex: cell cycle properties and regulation by physiological stimuli and injury. *Glia* **59**, 869-881 (2011).

9. Young, K.M. *et al.* Oligodendrocyte dynamics in the healthy adult CNS: evidence for myelin remodeling. *Neuron* **77**, 873-885 (2013).

10. Emery, B. *et al.* Myelin gene regulatory factor is a critical transcriptional regulator required for CNS myelination. *Cell* **138**, 172-185 (2009).

11. Koenning, M. *et al.* Myelin gene regulatory factor is required for maintenance of myelin and mature oligodendrocyte identity in the adult CNS. *J Neurosci* **32**, 12528-12542 (2012).

12. Hornig, J. *et al.* The transcription factors Sox10 and Myrf define an essential regulatory network module in differentiating oligodendrocytes. *PLoS Genet* **9**, e1003907 (2013).

13. McKenzie, I.A. *et al.* Motor skill learning requires active central myelination. *Science* **346**, 318-322 (2014).

14. Volkmar, F.R. & Greenough, W.T. Rearing complexity affects branching of dendrites in the visual cortex of the rat. *Science* **176**, 1445-1447 (1972).

15. Bliss, T.V. & Collingridge, G.L. A synaptic model of memory: long-term potentiation in the hippocampus. *Nature* **361**, 31-39 (1993).

16. Milner, B., Squire, L.R. & Kandel, E.R. Cognitive neuroscience and the study of memory. *Neuron* **20**, 445-468 (1998).

17. Lee, K.J., Rhyu, I.J. & Pak, D.T. Synapses need coordination to learn motor skills. *Rev Neurosci* **25**, 223-230 (2014).

18. Xu, T. *et al.* Rapid formation and selective stabilization of synapses for enduring motor memories. *Nature* **462**, 915-919 (2009).

19. Li, Q., Brus-Ramer, M., Martin, J.H. & McDonald, J.W. Electrical stimulation of the medullary pyramid promotes proliferation and differentiation of oligodendrocyte progenitor cells in the corticospinal tract of the adult rat. *Neurosci Lett* **479**, 128-133.

20. Gibson, E.M. *et al.* Neuronal activity promotes oligodendrogenesis and adaptive myelination in the mammalian brain. *Science* **344**, 1252304 (2014).

21. Freeman, S.A. *et al.* Acceleration of conduction velocity linked to clustering of nodal components precedes myelination. *Proc Natl Acad Sci USA* **112**, E321-328 (2015).

22. Funfschilling, U. *et al.* Glycolytic oligodendrocytes maintain myelin and long-term axonal integrity. *Nature* **485**, 517-521 (2012).

23. Lee, Y. *et al.* Oligodendroglia metabolically support axons and contribute to neurodegeneration. *Nature* **487**, 443-448 (2012).

24. Greiner-Tollersrud, L., Berg, T., Stensland, H.M., Evjen, G. & Greiner-Tollersrud, O.K. Bovine brain myelin glycerophosphocholine choline phosphodiesterase is an alkaline lysosphingomyelinase of the eNPP-family, regulated by lysosomal sorting. *Neurochem Res* **38**, 300-310 (2013).

25. Sakagami, H. *et al.* Biochemical and molecular characterization of a novel choline-specific glycerophosphodiester phosphodiesterase belonging to the nucleotide pyrophosphatase/phosphodiesterase family. *J Biol Chem* **280**, 23084-23093 (2005).

26. Morita, J. *et al.* Structure and biological function of ENPP6, a choline-specific glycerophosphodiester-phosphodiesterase. *Sci Rep* **6**, 20995. doi: 10.1038/srep20995

27. Zhang, Y. *et al.* An RNA-sequencing transcriptome and splicing database of glia, neurons, and vascular cells of the cerebral cortex. *J Neurosci* **34**, 11929-11947 (2014).

28. Hughes, E.G., Kang, S.H., Fukaya, M. & Bergles, D.E. Oligodendrocyte progenitors balance growth with self-repulsion to achieve homeostasis in the adult brain. *Nat Neurosci* **16**, 668-676 (2013).

29. Jolly, S., Fudge, A., Pringle, N., Richardson, W.D. and Li, H. (2016). Combining double fluorescence in situ hybridization with immunolabelling for detection of the expression of three genes in mouse brain sections. *J Vis Exp* e53976, doi:10.3791/53976.

30. Walker, M.P., Brakefield, T., Morgan, A., Hobson, J.A. & Stickgold, R. Practice with sleep makes perfect: sleep-dependent motor skill learning. *Neuron* **35**, 205-211 (2002).

31. Trapp, B.D., Nishiyama, A., Cheng, D. & Macklin, W. Differentiation and death of premyelinating oligodendrocytes in developing rodent brain. *J Cell Biol* **137**, 459-468 (1997).

32. Chang, A., Tourtellotte, W.W., Rudick, R. & Trapp, B.D. Premyelinating oligodendrocytes in chronic lesions of multiple sclerosis. *N Engl J Med* **346**, 165-73 (2002).

33. Matsumoto, Y. *et al.* Differential proliferation rhythm of neural progenitor and oligodendrocyte precursor cells in the young adult hippocampus. *PLoS One* **6**, e27628 (2011).

34. Bellesi, M. Sleep and oligodendrocyte functions. *Curr Sleep Med Rep* **1**, 20-26 (2015).

35. van Heyningen, P., Calver, A.R. & Richardson, W.D. Control of progenitor cell number by mitogen supply and demand. *Curr Biol* **11**, 232-241 (2001).

36. Draganski, B. *et al.* Neuroplasticity: changes in grey matter induced by training. *Nature* **427**, 311-312 (2004).

37. Scholz, J., Klein, M.C., Behrens, T.E. & Johansen-Berg, H. Training induces changes in white-matter architecture. *Nat Neurosci* **12**, 1370-1371 (2009).

38. Hu, Y. *et al.* Enhanced white matter tracts integrity in children with abacus training. *Hum Brain Mapp* **32**, 10-21 (2011).

39. Sampaio-Baptista, C. *et al.* Motor skill learning induces changes in white matter microstructure and myelination. *J Neurosci* **33**, 19499-19503 (2013).

40. Sagi, Y. *et al.* Learning in the fast lane: new insights into neuroplasticity. *Neuron* **73**, 1195-1203 (2012).

41. Ho, V.M., Lee, J.A. & Martin, K.C. The cell biology of synaptic plasticity. *Science* **334**, 623-628 (2011).

42. Kole, K. Experience dependent plasticity of the neurovasculature. *J Neurophysiol* **114**, 2077-2079 (2014).

43. Makinodan, M., Rosen. K.M., Ito, S. & Corfas, G. A critical period for experience-dependent oligodendrocyte maturation and myelination. *Science* **337**, 1357-1360 (2012).

44. Mangin, J.M., Li, P., Scafidi, J. & Gallo, V. Experience-dependent regulation of NG2 progenitors in the developing barrel cortex. *Nat Neurosci* **15**, 1192-1194 (2012).

45. Bergles, D.E. and Richardson, W.D. (2015). Oligodendrocyte development and plasticity. In Glia; Cold Spring Harbor Laboratory Press (Cold Spring Harbor) (eds BA Barres, MR Freeman, B Stevens). pp139-165. *Cold Spring Harb Perspect Biol* 8 doi: 10.1101/cshperspect.a020453

46. Hines, J.H., Ravanelli, A.M., Schwindt, R., Scott, E.K. & Appel, B. Neuronal activity biases axon selection for myelination in vivo. *Nat Neurosci* **18**, 683-689 (2015).

47. Mensch, S. *et al.* Synaptic vesicle release regulates myelin sheath number of individual oligodendrocytes in vivo. *Nat Neurosci* **18**, 628-630 (2015).

Fig. 1 Time course of motor skill learning in mice and the requirement for *Myrf*. (**a**) Average speeds on complex wheel (pictured) during successive 24 hour intervals. *P-Myrf* $^{-/-}$ mice (n=32, 17 male) performed less well then their *P-Myrf* $^{+/-}$ littermates (n=36, 20 male) over all 8 days of the experiment, including the first 24 hour interval. (**b**) Average speeds during successive 2 hour intervals during the first 3 days of the experiment. Most improvement during night 1 occurred during the first 4 hours, both for *P-Myrf* $^{+/-}$ and *P-Myrf* $^{-/-}$ animals. At the beginning of nights 2 and 3, the mice ran faster from the outset than at any time during the preceding 24 hours. (**c**) Average speeds in 20 minute intervals during the first 4 hours of the first night. The performance of *P-Myrf* $^{+/-}$ and *P-Myrf* $^{-/-}$ mice increased from the same low level during the first 1-2 hours, diverging significantly within 2-4 hours' exposure to the complex wheel. Data were analyzed by two-way ANOVA with Bonferroni's post-hoc test. In (**b**), each night was treated separately for multiple comparisons. Error bars indicate s.e.m. $*p < 0.05$, $**p < 0.01$, $***p < 10^{-3}$, $****p < 10^{-4}$. [(**a**) Night 1: p=0.09, t=2.5. Night 2: p=0.01, t=3.3. Night 3: p=0.004, t=3.5. Night 4: p=0.004, t=3.5. Night 5: p=0.0009, t=3.9. Night 6: p<0.0001, t=4.6. Night 7: $p<10^{-4}$, t=4.7. Night 8: p=0.001, t=3.8. F(1,497)=109.9 and degrees of freedom (df)=497 throughout.] [(**b**) Night 1: 2 h, p=0.43, t=1.81; 4 h, p=0.03, t=2.8; 6 h, p=0.009, t=3.2; 8 h, p=0.004, t=3.4; 10 h, p=0.002, t=3.7; 12 h, p=0.004, t=3.5. F(1,396)=56.2. Night 2: 2 h, p=0.007, t=3.3; 4 h, p=0.003, t=3.5; 6 h, p=0.063, t=2.6; 8 h, p=0.015, t=3.0; 10 h, p=0.11, t=2.4; 12 h, p=0.03, t=2.8. F(1,396)=51.1. Night 3: 2 h, p=0.002, t=3.63; 4 h, p=0.004, t= 3.43; 6 h, p=0.02, t= 2.95; 8 h, p=0.072, t=2.53; 10 h, p=0.>0.99, t=1.054; 12 h, p=0.24, t=2.06. F(1,396)=40.79. df=396 throughout.] [(**c**) 20 min: p>0.99, t=0.69; 40 min: p>0.99, t=0.10; 60 min: p>0.99, t=0.13; 80 min: p>0.99, t=0.81; 100 min: p>0.99, t=1.41; 120 min: p=0.30, t=2.44; 140 min: p=0.022, t=3.12; 160 min: p=0.10, t=1.83; 180 min: p=0.83, t=2.63; 200 min: p=0.14, t=2.63; 220 min: p=0.017, t=3.21; 240 min: p=0.095. F(1,792)=42.32 and df=792 throughout.]

Fig. 2 Oligodendrocyte dynamics during motor skill learning. (**a**) Experimental design: all mice (approximately equal numbers of male and female) were given tamoxifen by gavage on 4 successive days (P60 to P63 inclusive), then EdU was administered in the drinking water for 10 days (P75 to P84) before transferring the mice to cages equipped with a complex wheel for up to 8 days. (**b**) Subcortical white matter of wild type mice housed with a wheel for 8 days ("8-day runners"). The great majority (~97%) of EdU^+ cells were also $Sox10^+$ oligodendrocyte lineage cells. At this time point there is a mixture of CC1-negative presumptive OPs (arrowhead) and $CC1^+$ newly-formed oligodendrocytes (arrows). Images are representative of >3 similar experiments. (**c**,**d**) Numbers of newly-generated (EdU^+) oligodendrocyte lineage cells at different developmental stages in 2-day runners versus control littermates, housed without a wheel ("non-runners"). The

number of EdU^+ $CC1^+$ newly-formed oligodendrocytes is the same in 2-day runners and non-runners, both in motor cortex (**c**) and underlying white matter (WM) (**d**). The number of recently generated OPs (EdU^+ $Pdgfra^+$) is decreased in 2-day runners compared to non-runners, with a reciprocal increase in the number of newly-differentiating oligodendrocytes (EdU^+ $Pdgfra^-$ $CC1^-$). (**e**,**f**) Production of (EdU^+ $CC1^+$) new myelinating oligodendrocytes is accelerated in both motor cortex (**e**) and subcortical white matter (**f**) of runners versus non-runners. The new oligodendrocytes accumulate between 4 and 8 days running. The number of new oligodendrocytes is strongly reduced in *P-Myrf* $^{-/-}$ mice, both runners and non-runners, compared to wild type mice (non-runner 8 days, Motor cortex: p=0.00091, t= –4.71, df=9; Sub-cortical white matter: $p<10^{-5}$, t= –15.43, df=9; n=6 for wild type mice, n=5 for *Myrf* $^{-/-}$ mice). (**g**) Production of new myelinating oligodendrocytes (EdU^+ $CC1^+$) in the optic nerve is not increased by running (p=0.71, t= –0.39, df=9, n=5 runners, n=6 non-runners). All data from runners versus non-runners were compared by two-tailed unpaired *t*-test. Error bars indicate s.e.m. $*p < 0.05$, $**p < 0.01$, $***p < 0.001$. Scale bar in **b**: 40 μm.

[(**c**) $CC1^+$, p=0.81, t= –0.25; $Pdgfra^+$, p= 0.012, t=3.1; $Pdgfra^-$, $CC1^-$, p=0.012, t= –3.1, df=10, n=6 mice] [(**d**) $CC1^+$, p= 0.90, t= –0.13; $Pdgfra^+$, p=0.014, t=2.94; $Pdgfra^-$, $CC1^-$, p=0.012, t=3.07, df=10. n=6 mice.] [(**e**) 2 day, p=0.90, t= –0.13, df=10, n=6 mice each group; 4 days, p=0.027, t= –2.90, df=6, n=4 mice each group; 6 days, p=0.0039, t= –3.73, df=10, n=6 mice each group; 8 days (WT), p=0.0006, t= –5.0, df=10, n=6 mice each group; 8 days (*Myrf* $^{-/-}$), p=0.18, t= –1.47, df=8, n=6 mice each group.] [(**f**) 2 days, p=0.61, t= –0.53, df=10; n=6 mice each group; 4 days, p=0.003, t= –4.8, df=6, n=4 mice each group; 6 days, p=0.0027, t= –3.54, df=10, n=6 mice each group; 8 days (WT), p=0.0007, t= –4.82, df=10, n=6 mice each group; 8 days (*Myrf* $^{-/-}$), p=0.61, t= –0.53, df=8, n=5 mice each group.]

Fig. 3 *Enpp6* marks newly-forming, pre-myelinating oligodendrocytes. (**a**) RNA-seq data adapted from reference 27, http://web.stanford.edu/group/barres_lab/brain_rnaseq.html *Enpp6* is expressed highly in newly-formed oligodendrocytes (OLs) and less so in myelinating oligodendrocytes. *FPKM*: fragments per kilobase of transcript per million mapped reads, but not in OPs or other neural cells. (**b**) ISH for *Mbp* transcripts on sections of P90 mouse motor cortex reveals many small cell bodies of mature oligodendrocytes (arrowheads) and a few larger process-bearing "spidery" cells (arrows), resembling "pre-myelinating" oligodendrocytes described previously[31,32]. (**c**) Double ISH for *Mbp* and *Enpp6* shows that the spidery Mbp^+ cells (arrows) are also $Enpp6^+$. Under our ISH conditions (Supplementary Fig. 2) all *Enpp6* ^{high} cells are spidery Mbp^+ cells and vice versa; they represent ~5% of all Mbp^+ cells in both grey and white matter at P90. (**d**) The spidery Mbp^+ cells can be recognized in both cortical grey matter and white matter at P90, although

the high density of *Mbp*$^+$ mature oligodendrocytes tends to obscure them in white matter. The right panels of (D) and (E) are higher-magnification images of the areas indicated on the left. (**e**) In *P-Myrf*$^{-/-}$ brain at P90 there are almost no *Mbp*$^+$ spidery cells in grey or white matter, identifying them as newly-forming oligodendrocytes. SCWM, sub-cortical white matter. Images are representative of >3 similar experiments. Error bars in (**a**) are s.e.m. Scale bars: (**b**,**c**) and (**d** right, **e** right) 50 μm, (**d** left, **e** left) 200 μm.

Fig. 4 *Enpp6*^{high}, *Mbp*$^+$ newly-formed oligodendrocytes express myelin structural proteins and synthesize myelin. (**a**) ISH for *Enpp6* (left) followed by double immunolabeling for Mag (middle) and Mbp (right) demonstrates that a significant fraction (~45%) of *Enpp6*^{high} cells synthesize myelin sheaths in the P10 cortical grey matter. (**b**) Double ISH for *Enpp6* (left) and *Mbp* (middle, green) followed by immunolabeling for Mbp (right, red) confirms that some *Enpp6*^{high}, *Mbp*$^+$ newly-formed oligodendrocytes synthesize Mbp protein and myelin in the P10 cortex. *Mbp* mRNA is present in the cell body, radial processes and nascent myelin sheaths. (**c**,**d**) At P90, double ISH for *Enpp6* and *Mbp* (green) followed by immunolabeling for Mbp (red) also identifies *Enpp6*$^+$ cells in the motor cortex that are synthesizing myelin sheaths (arrow in **c**). The cell shown is in cortical layer 2; around 60% of *Enpp6*^{high} cells in this region of the cortex, where myelin sheaths are relatively sparse, were associated with myelin. (**d**) Higher magnification images of the myelin sheath indicated by an arrowhead in (**c**, middle). "Spots" of *Mbp* mRNA (green) are visible in (**d**) where there is no Mbp$^+$ myelin sheath (red); presumably these represent oligodendrocyte processes that are in contact with axons but have not yet translated myelin proteins (i.e. nascent myelin sheaths). Images are representative of >3 similar experiments. Scale bars: 50 μm.

Fig. 5 Visualization of *Enpp6*^{high} cells in the developing mouse forebrain by ISH. *Enpp6*^{high} cells are much less numerous in P90 forebrain compared to *Plp*$^+$ or *Mbp*$^+$ mature oligodendrocytes (compare **a**,**b**,**g**). They are also less numerous and differently distributed to *Pdgfra*$^+$ OPs (compare **c**,**g**). *Enpp6*^{high} cells are very infrequent in *P-Myrf*$^{-/-}$ brains compared to wild type (**d**,**g**), consistent with their being early-differentiating oligodendrocytes; *Myrf*$^{-/-}$ OPs fail to differentiate but die as nascent oligodendrocytes[10]. (**e**–**h**) As expected for newly-differentiating oligodendrocytes, *Enpp6*^{high} cells are more abundant in the white and gray matter at earlier ages when oligodendrocyte generation and myelination is more active. Significant numbers are still present in young adults at P90 (arrows in **g**). Even at one year of age (**h**) there are small numbers of *Enpp6*^{high} cells (arrows). Images are representative of >3 similar experiments. Scale bar, 100 μm.

Fig. 6 Rapid increase in *Enpp6* ^{high} newly-forming oligodendrocytes in response to motor skill learning. (**a**–**i**) ISH for *Enpp6* in sections of non-runner, runner (24 hours with the complex wheel) and *P-Myrf* $^{-/-}$ (non-runner) subcortical white matter (**a**–**f**) or motor cortex (**g**–**i**). (**d**–**f**) are higher-magnification images of the areas indicated in (**a**–**c**). There is a noticeable increase in the number of strongly-labeled cells in runners relative to non-runners, both in motor cortex (compare **g**,**h**) and subcortical white matter (compare **a**,**b** and **d**,**e**). (**j**,**k**) Quantification of *Enpp6* ^{high} cells in wild type or *P-Myrf* $^{-/-}$ mice housed with or without a complex wheel for different times. Numbers of *Enpp6* ^{high} cells were increased in runners versus non-runners within only 2.5 hours in the sub-cortical white matter and within 4 hours in motor cortex and persisted for at least 8 days, in both white and grey matter. Numbers of *Enpp6* ^{high} cells were greatly decreased in *P-Myrf* $^{-/-}$ compared to wild type mice, [non-runner 12 h, (**j**) Motor cortex: $p<10^{-5}$, t= –13.37, df=12; (**k**) Sub-cortical white matter: $p<10^{-5}$, t= –11.28, df=12; n=10 for wild type mice, n=4 for *Myrf* $^{-/-}$ mice]. Data from runners and non-runners were compared by two-tailed unpaired *t*-test. Error bars indicate s.e.m. *$p < 0.05$, **$p < 0.01$, ***$p < 0.001$, comparing runners with non-runners. WM, white matter. Images are representative of >3 similar experiments. Scale bars: (**a**–**c**), 200 μm; (**d**–**i**), 100 μm.

[(**j**) 2.5 h, p=0.43, t= –0.81,df=15, n=8 mice for non runners, n=9 mice for runners; 4 h, $p=9x10^{-5}$, t= –5.024, df=18, n=10 mice each group; 12 h (wild type), $p<10^{-5}$, t= –8.50, df=18, n=10 mice each group; 24 h, p=0.00019, t= –6.46, df=8, n=5 mice each group; 48 h, p=0.0038, t=4.03, df=9, n=4 mice for non runners, n=6 for runners; 8 d, p=0.0013, t= –4.42, df=10, n=6 mice each group; 12 h (*Myrf* $^{-/-}$), p=0.049,t= –2.59, df=5, n=4 mice for non runners, n=3 mice for runners.] [(**k**) 2.5 h, p=0.0026, t= –3.60, df=15, n=8 mice for non runners, n=9 mice for runners; 4 h, p= 0.0026, t= –3.50, df=18, n=10 mice each group; 12 h (wild type), $p<10^{-5}$, t= –6.20, df=18, n=10 mice each group; 24 h, p=0.001, t= –5.06, df=8, n=5 mice each group; 48 h, p=0.0038, t=4.03, df=8, n=4 mice for non runners, n=6 for runners; 8 d, $p=2x10^{-5}$, t= –5.71, df=10, n=6 mice each group; 12 h (*Myrf* $^{-/-}$), p=0.013, t= –3.77, df=5, n=4 mice for non runners, n=3 mice for runners.]

Fig 7 Increased production of *Enpp6*$^{+}$ new-formed oligodendrocytes is a response to motor learning, not physical exercise. (**a**) Experimental design. One group of mice self-trained on the complex wheel for one week, rested for 2 weeks then was re-introduced to the wheel along with a separate group that was introduced for the first time. After 24 hours (P85-86) both groups of mice (and parallel groups of non-runners) were analyzed by ISH for *Enpp6*. Despite the fact that pre-trained mice ran faster and further than the "first-timers" (**b**,**c**), there was an increase in the number density of *Enpp6* ^{high} newly-formed oligodendrocytes in the first timers but not in the pre-trained group, both in motor cortex (**d**) and subcortical white matter (**e**). Elevated oligodendrocyte

production was not observed in the visual cortex (**f**), demonstrating regional specificity. All data were compared by two-tailed unpaired *t*-test. n=4 mice in each group. Error bars indicate s.e.m. **p* < 0.05, ***p* < 0.01, ****p* < 0.001. [(**b**) $p=10^{-5}$, t= –11.72, df=6.] [(**c**) p=0.00035, t= –7.23, df=6.] [(**d**) 1st, p=0.00033, t= –7.29, df=6; 2nd, p=0.38, t= –0.95, df=6.] [(**e**) 1st, p=0.0021, t= –5.16, df=6; 2nd, p=0.34, t= –1.03, df=6.] [(**f**) p=0.80, t=0.27 df=6.]

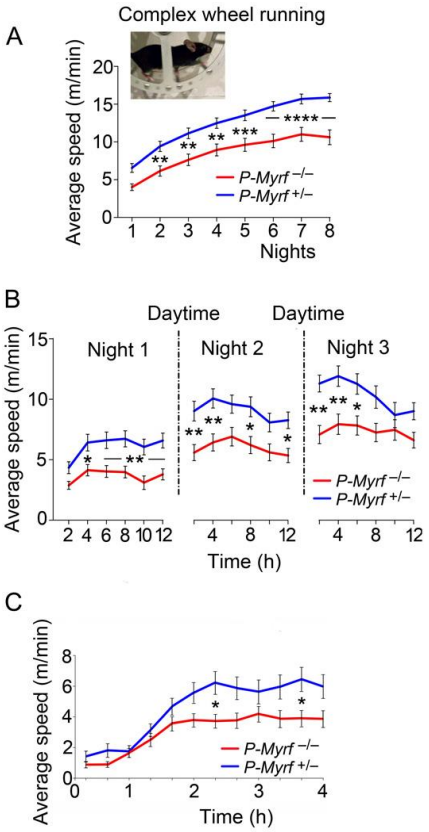

Figure 1

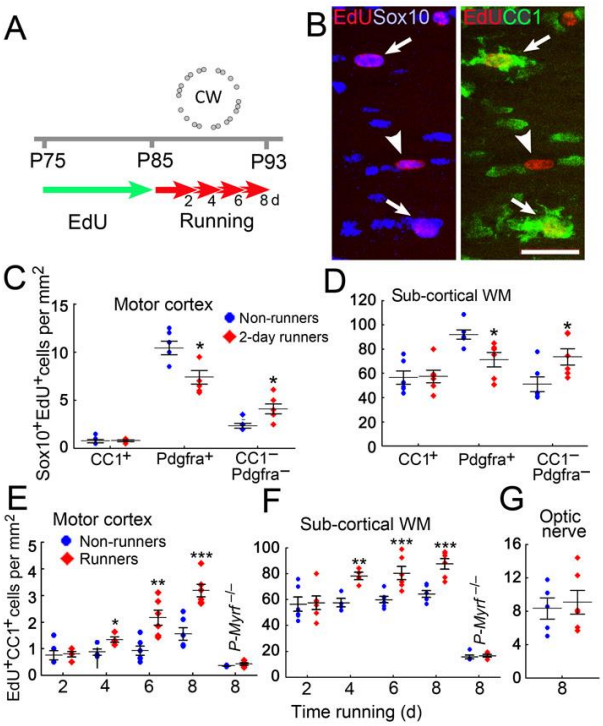

Figure 2

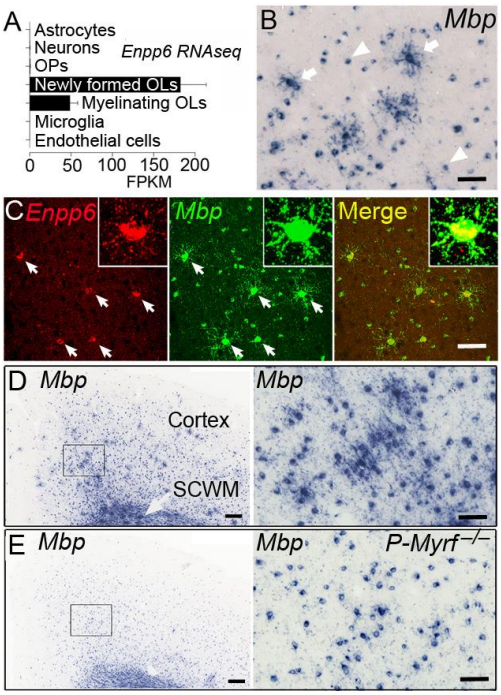

Figure 3

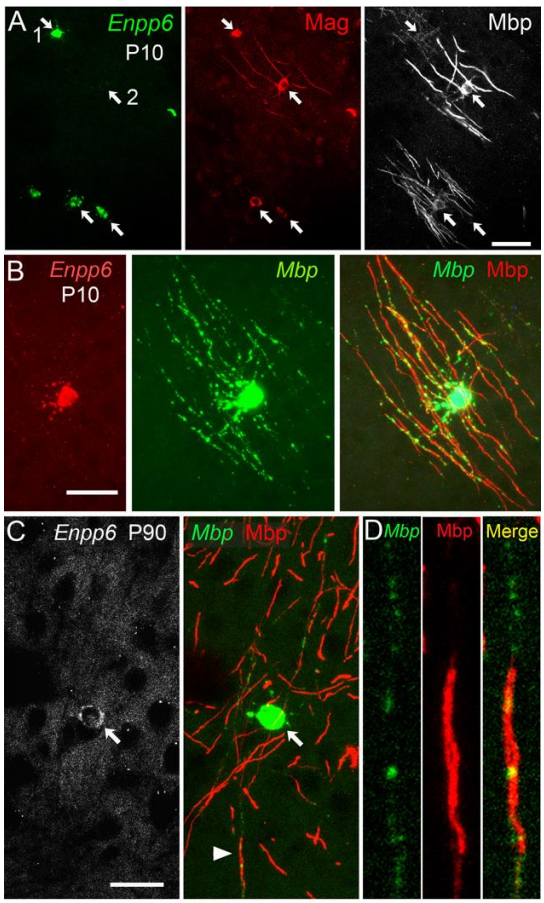

Figure 4

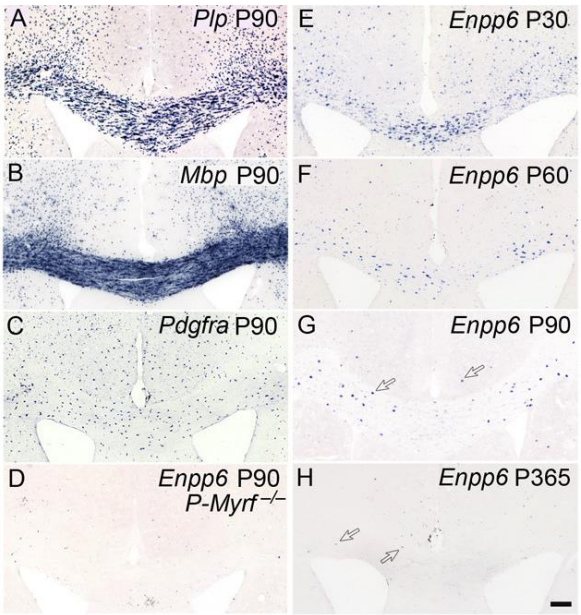

Figure 5

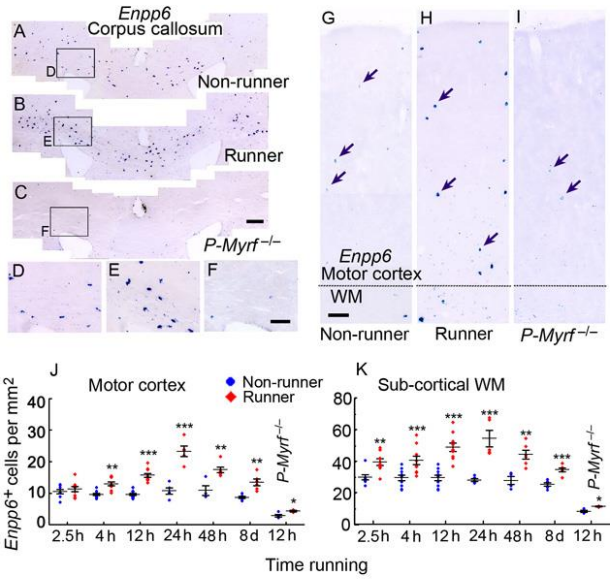

Figure 6

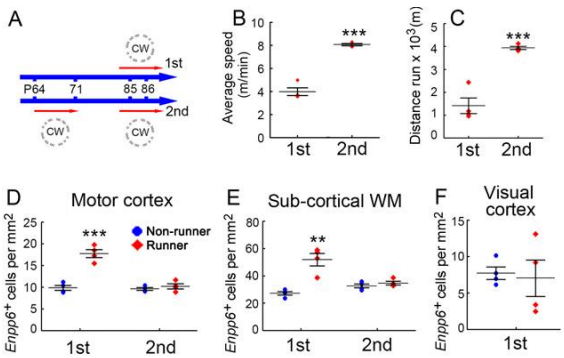

Figure 7

Methods

Mice

Myrf$^{flox/flox}$ mice were imported to UCL originally (in 2010) on a mixed 129/CBA/C57B6 background. After crossing into a homozygous *Pdgfra-CreER*^{T2} background (predominantly C57B6; 3 generations) they have been maintained by sibling crosses for more than 6 generations and now generate exclusively agouti offspring. They are therefore mixed C57B6/CBA/129 with the major contribution being C57B6 (though agouti coat-colour is CBA-derived). Generation and genotyping of *Pdgfra-CreER*^{T2} *: Myrf* $^{flox/flox}$ and *Pdgfra-CreER*^{T2}*: Myrf* $^{+/flox}$ littermates has been described[13]. Tamoxifen (Sigma) was dissolved at 40 mg/ml in corn oil by sonicating at 21°C for one hour. It was administered to mice (both *Myrf* $^{flox/flox}$ and *Myrf* $^{+/flox}$) by oral gavage on four consecutive days ending on P64 (4 cohorts) or P94 (1 cohort) to induce recombination and deletion of *Myrf* in Pdgfra^{+} OPs (each dose was 300 mg/Kg body weight). This generated *P-Myrf* $^{-/-}$ and *P-Myrf* $^{+/-}$ mice for behavioural experiments. Mice were rested 3 weeks between the last tamoxifen dose and being introduced to the complex wheel at P85 or P115 (reference 13). Wild type mice were C57B6 (Charles River, Margate, UK). All animal experiments were pre-approved by the UCL Ethical Committee and authorized by the Home Office of the UK Government.

The complex wheel

We purchased wheel cages (Lafayette Neuroscience) that allow digital recording of wheel rotation speed over time (using an infra-red beam) for more than 20 cages simultaneously. Complex wheels were made by removing 16 rungs from 38-rung, 12.7 cm diameter regular wheels, creating a 19-rung repeating pattern[13]. Mice were maintained on a 12-hour artificial light-dark cycle, caged singly with the wheel and a small amount of nesting material (tissue paper). During running experiments, food and water was replenished every 48 hours (during the light/ inactivity cycle) but otherwise the mice were not disturbed. For comparison of *P-Myrf* $^{-/-}$ and *P-Myrf* $^{+/-}$ mice, wheel speed was measured once per hour during the light/ inactive period and at one-minute intervals during the dark/ active period and data were exported automatically to a spreadsheet. Average wheel speeds were calculated for successive time intervals (12 hours, 2 hours or 20 minutes) and compared by two-way ANOVA with Bonferroni's post-hoc tests using GraphPad Prism 6.0 software.

Histology and cell counts

Mice were perfusion-fixed with 4% (w/v) paraformaldehyde (PFA; Sigma) in diethylpyrocarbonate (DEPC) treated phosphate-buffered saline (PBS). Brain tissue was dissected and post-fixed in 4%

PFA overnight at 4°C. Tissue was cryoprotected in 20% (w/v) sucrose (Sigma) in PBS before freezing in OCT on the surface of dry ice. Coronal cryosections (20 μm) of the brain were collected and processed as floating sections. Primary and secondary antibodies were diluted in blocking solution (0.1% [v/v] Triton X-100, 10% [v/v] fetal calf serum in PBS) and applied to sections overnight at 4°C. Primary antibodies were anti-PDGFRa (rabbit, New England Biolabs catalogue number 3164S, 1:500 dilution), anti-Olig2 (rabbit, Abcam AB9610, 1:400), anti-Sox10 (guinea pig, 1:2000; a gift from M.Wegner), monoclonal CC1 (mouse, Calbiochem OP80,1:200), anti-Mag (mouse, Abcam ab89780, 1:200) and anti-Mbp (rat, AbD Serotec MCA409S, 1:200).

Low-magnification (20x objective) confocal images were collected using a Leica SPE laser scanning confocal microscope as Z-stacks with 1 μm spacing, using standard excitation and emission filters for DAPI, FITC (Alexa Fluor-488), TRITC (Alexa Fluor-568) and Far Red (Alexa Fluor-647). Cells were counted in non-overlapping fields of coronal sections of the corpus callosum or motor cortex, between the dorsolateral corners of the lateral ventricles (6 fields per section, three sections from each of three or more mice of a given experimental group).

EdU labeling in vivo

Mice were given 5-ethynyl-2'-deoxyuridine (EdU) in their drinking water (0.2 mg/ml)[9] for 10 days from P75-P85. The animals were caged with a complex wheel for different times and then were perfusion fixed and analyzed by immunolabeling floating cryosections (20 μm) with monoclonal CC1, anti-Sox10, and anti-Pdgfra followed by detection of EdU using the AlexaFluor-555 Click-iT detection kit (Invitrogen).

In situ hybridization

Our in situ hybridization (ISH) protocols are available at http://www.ucl.ac.uk/~ucbzwdr/Richardson.htm and reference 29. Briefly, digoxigenin (DIG)- or fluorescein (FITC)-labelled RNA probes were transcribed in vitro from cloned cDNAs for mouse *Mbp* (DIG or FITC), *Pdgfra* (FITC) and *Enpp6* (DIG). For single probe ISH, the DIG or FITC signal was visualized with alkaline phosphatase (AP)-conjugated anti-DIG or -FITC Fab2 fragments and a mixture of nitroblue tetrazolium (NBT) and 5-bromo-4-chloro-3-indolyl phosphate (toluidine salt) (BCIP) (all reagents from Roche Molecular Biochemicals). For double fluorescence ISH, two probes – one FITC labelled and the other DIG labelled – were applied to sections simultaneously. The FITC signal was visualized by tyramide signal amplification (TSA) fluorescent system (NENTM Life Science Products, Boston) according to the manufacturer's instructions using Horseradish Peroxidase (HRP) conjugated anti-FITC-POD antibody. After that,

the DIG signal was visualized by a Fast Red fluorescence system (Roche) according to the manufacturer's instructions using AP-conjugated anti-DIG Fab2 antibody. For combined immunolabelling/ ISH, immunolabeling was carried out after the ISH signal had been developed using Fast Red or TSA. For Mag and Mbp immunolabeling after ISH, the sections were heated at 95°C for 20 minutes in 0.01 M citrate acid buffer (in di-ethyl pyrocarbonate treated water) before incubating with the *Enpp6* probe, then developing the signal with tyramide. After blocking with normal goat serum, the sections were incubated with rat anti-Mbp and mouse anti-Mag for 3 days at 4°C before the secondary antibodies (AlexaFluor-647 anti-rat IgG and AlexaFluor-568 anti-mouse IgG). For double *Enpp6* and *Mbp* ISH followed by Mbp immunolabeling, the *Mbp* signal was first developed using TSA, then the *Enpp6* signal with Fast Red, then the anti-Mbp was added for 3 days at 4°C before the AlexaFluor-647 anti-rat IgG.

Statistics

No statistical methods were used to pre-determine sample sizes but our sample sizes are similar to those reported in previous publications [8,18,31]. Mice were randomly assigned to experimental groups (e.g. runners or non-runners) with approximately equal numbers of female and male mice in each group. Prism 6.0 software (GraphPad) was used for statistical analysis. Running wheel data were analyzed by calculating average speed (m/ minute) for individual mice over different time windows, then mean ± s.e.m. for the whole experimental group over the same period. To assess differences between experimental cohorts at a given point in a time series (Fig. 1, Supplementary Fig. 1) we used two-way ANOVA with Bonferroni's post-hoc tests. For comparing experimental cohorts at a single time point (Figs. 2, 6, 7) we used the two-tailed unpaired t-test. Cell counts are displayed as mean ± s.e.m. All cell counts in Figs. 2, 6 and 7 were carried out by L.X., blind as to whether the mice were runners or non-runners. For key experiments (Fig. 6j,k; 2.5 hour, 4 hour and 12 hour time points) cells were also counted independently by W.D.R., blinded, with similar results (not shown). Data from runners and non-runners were compared by two-tailed unpaired *t*-test using GraphPad Prism 6.0. The variances of each pair of data-sets being compared were similar to each other and consistent with their being normally-distributed (assessed by Kolgomorov-Smirnov test: http://www.physics.csbsju.edu/stats/KS-test.n.plot_form.html). No animals or data points were excluded from the analysis.

Data availability

The data that support the findings of this study are available from the corresponding author on request.